Semi-annual Technical Report
for the Period 1/1/72 - 6/30/72

Conduction Mechanisms in Thick Film Microcircuits

Grant Number: DAHC15-70-G7

ARPA Order No.: 1642

Grantee: Purdue Research Foundation

Principal Investigator: R. W. Vest
(317) 494-4445

Effective Date of Grant: 7/1/70

Grant Expiration Date: 6/30/73

Amount of Grant: $181,260

August 1, 1972

Forward

The research described in this report constitutes the fourth six months effort under a grant from the Advanced Research Projects Agency, Department of Defense under the technical cognizance of Dr. Norman Tallan, Aerospace Research Laboratories, United States Air Force. The research was conducted in the Turner Laboratory for Electroceramics, School of Electrical Engineering and School of Materials Science and Mettallurgical Engineering, Purdue University, West Lafayette, Indiana 47907, under the direction of Professor R. W. Vest. Contributing to the project were Visiting Assistant Professor G. L. Fuller, Mr. D. J. Deputy, Mr. R. L. Reed, Mr. K. N. Sheely, Jr., Mr. P. S. Wang, and Mr. J. L. Wright.

ABSTRACT

Preliminary results on resistor microstructure are presented and their correlation with the proposed model discussed. The study of RuO_2-glass composites led to the conclusion that the difference in thermal expansion between the RuO_2 and the glass is a minor factor in controlling resistor TCR. Preliminary studies of the resistance changes during firing of a thick film resistor are described. Evaluation of the performance of the screen printing machine has established that the variations in resistor value which can be expected from this phase of the process will be less than $\pm$ 5%.

TABLE OF CONTENTS

LIST OF FIGURES

LIST OF TABLES

I. Introduction

The current status of thick film technology as applied to conductive and resistive formulations is largely the result of empirical developments. The development of new materials as well as the improvement of existing systems have been hindered by an inadequate understanding of the mechanisms by which electric charge is transported in thick film resistors and conductors.

One of the factors that any model for conduction in thick film microcircuits must explain is the fact that the temperature coefficient of resistance (TCR) of a resistor is much lower than the TCR of any of the individual ingredients from which it was made. Several possible approaches to explaining this "TCR anomaly" which are being explored in this project are:

1. Changes in contact resistance between adjacent particles due to thermal stresses,
2. Changes in the intrinsic properties of the conductive material during processing,
3. Formation of new phases which contribute to the conduction,
4. Size effects which change the intrinsic properties of the conductive,
5. Changes in the geometry factor with temperature.

Published work concerning these possible mechanisms was discussed in the first report on this project [1].

The primary thrust of the experimental program is to relate the electrical properties of the thick films to the material properties and processing conditions through microstructure. The materials properties to be correlated are: resistivity; temperature coefficient of resistivity; coefficient of thermal expansion; interfacial energy; particle shape, size, and size distribution; and chemical reactivity with other constituents. The processing conditions to be correlated are time, temperature, and atmosphere during firing.

The specific objectives of the program are:

1. Determine the dominant sintering mechanisms responsible for microstructure development, and establish the relative importance of the various properties of the ingredient materials.
2. Determine the dominant mechanisms limiting electrical charge transport, and establish the relative importance of the various properties of the ingredient materials.
3. Develop phenomenological models to inter-relate the various material properties with system performance.

A proposed model to satisfy objective 1 above was presented in the previous report [2], and an experimental program has been developed to test the various aspects of the model. Preliminary microstructure results presented in this report are in agreement with the preditions of the model. Studies of RuO_2 - glass composites discussed in this report were undertaken in order to contribute to objective 2. The studies of screen printing presented in this report were required before work on objective 3 could begin.

II. Resistor Microstructure Studies

A. General

Thick film resistors are composite systems consisting of two or more phases. The electrically conducting phase (or phases) is present in the formulation as discrete particles (or as a homogeneous solution in the case of resinate systems), but must develop into a physically continuous network along the length of the resistor during the firing operation. One of the primary goals of this project is to relate the final microstructure and the kinetics of its formation to the physical properties of the ingredient materials. In the previous report [2] a model that is consistent with both current theories of ceramic microstructure development (sintering, etc.), and several observations commonly reported for thick-film resistor systems was presented. The model can be tested by direct observations via hot stage microscopy, and such a program has been initiated. In addition, the model predicts certain features in the microstructure of fired resistors, and efforts to investigate these features have been initiated.

The microstructure is being investigated through the use of both a scanning electron microscope and an optical microscope. Each instrument has certain advantages and disadvantages when applied to the RuO_2 - lead borosilicate glass resistor system. The primary advantages of the SEM are high magnification (up to 100,000 x) and a large depth of field. It can also be used in conjunction with an x-ray spectrometer to obtain chemical analyses of selected regions of the specimen. Its primary disadvantages

are the charging of poorly conducting regions of the specimen which limits the usable magnification and degrades the quality of the image, and the fact that rutherium is not easily distinguishable from the lead in the glass. The principle advantages of the optical microscope are the ease with which specimens can be observed, and the fact that the glass is optically transparent. Its major disadvantages are the small depth of field and the relatively low maximum magnification (1800x with an oil immersion objective lens).

B. Sample Preparation

In general, the thick film resistors under consideration consist of a network of ruthenium dioxide particles imbedded in a glass (63% PbO-25% B_2O_3 - 12% SiO_2) matrix, and the glass often masks the structure of the RuO_2, particularly for observations with the SEM. Attempts to apply standard metallographic procedures for producing specimens to be examined with the SEM were not successful. A resistor was sectioned with a low-speed diamond saw, followed by diamond disc polishing of the surface, and a final etch with HCl. Observations of this specimen showed that the resistor material and conductive had been smeared over the substrate, and no particular structure was seen. Because of the smearing problems, a fracture technique was attempted by sawing almost through the substrate below the resistor, and then breaking the piece. There was no evidence of smearing, but very few microstructural details of the RuO_2 network could be observed.

An ideal solution to the problem of the glass masking the microstructure would be to etch the resistor so as to remove some of the glass while leaving the RuO_2 unchanged. Ruthenium dioxide is quite inert, and is not soluble in most etchants, while the lead-borosilicate glass is readily attacked by

HCl, NaOH, and to some extent by HNO_3. Sodium hydroxide (concentrated-warm) is extremely reactive with the glass; for example, a resistor completely disappeared after being immersed for one minute in NaOH. Because of this very fast reaction, the concentrated NaOH solution is not a suitable etchant for exhibiting resistor microstructure. The preferred etchant appears to be HCl; etching high lead optical glass with HCl was one of the earliest methods of producing low reflection surfaces, apparently by leaching the lead from the glass surface and leaving behind a surface layer of SiO_x with a refractive index between that of the glass and air. An example of how HCl exposure influences the resistance of a particular resistor is shown by the following results:

Before HCl (concentrated) etch	R = 138 ohms.
After 15 min etch	R = 182 ohms.
After 30 min. etch	R = 279 ohms.

These and subsequent experiments have shown that for the sample preparation techniques studied the best results on microstructure using the SEM or the optical microscope with reflected light are obtained after heavy etching of the resistor with HCl. If the etching is sufficient, very little lead (in the glass) remains; X-ray spectra for a typical resistor after heavy etching show the presence of Ru, very little Pb, and a significant amount of Si.

Resistor microstructure can be studied using the optical microscope with transmitted light simple by thinning the substrate on a diamond grinding wheel to approximately 10 mils provided the resistor is sufficiently dilute in the conductive phase

C. Results and Correlation with Model

A test resistor was made with an RuO_2/glass ratio of 5/95 by weight (3.4 volume percent RuO_2/glass). The RuO_2/glass mixture was blended with the ethyl cellulose/butyl carbitol screening agent on a three roll mill, and manually printed on a 96% alumina substrate over Pt conductive pads. The resistor was dried at 220°C for 15 minutes followed by 45 minutes at 300°C. The resistor was then fired at a linear heating rate of 25°C/min to a peak of 810°C, held at 810°C for 8 minutes, and cooled at a rate of 75°C/min. The sheet resistance of this resistor was 100,000 ohms per square.

The resistor was broken into two parts, and one half was etched in 1:1 HCl for 5 minutes for observation with reflected light. The two photomicrographs of Figure 1 represent regions dilute and concentrated in RuO_2. The grey areas in the photomicrographs are regions rich in conductive, but which are out of focus due to the low depth of field at this magnification (720 x). The second half of the resistor was prepared for observation in transmitted light by grinding away the bottom of the substrate to a thickness of approximately 10 mils. The photomicrographs of Figure 2 show the RuO_2 network at four different magnifications (720x, 900x, 1080x, and 1800x). The highest magnification is at the ultimate resolving power of the microscope, but the general structure of the conductive network can be determined. Studies of this resistor with the SEM were not complete at the time of writing of this report.

The microstructure model [2] predicts that starting with the conductive particles dispersed among the glass particles and increasing temperature, the relative interfacial energies of the glass and the conductive cause the glass particles to sinter and flow together to form larger particles and neighboring conductive particles are pulled together by a thin layer of glass that forms on their surfaces. While in this configuration the conductive

Figure 1. Resistor Microstructure: Reflected Light

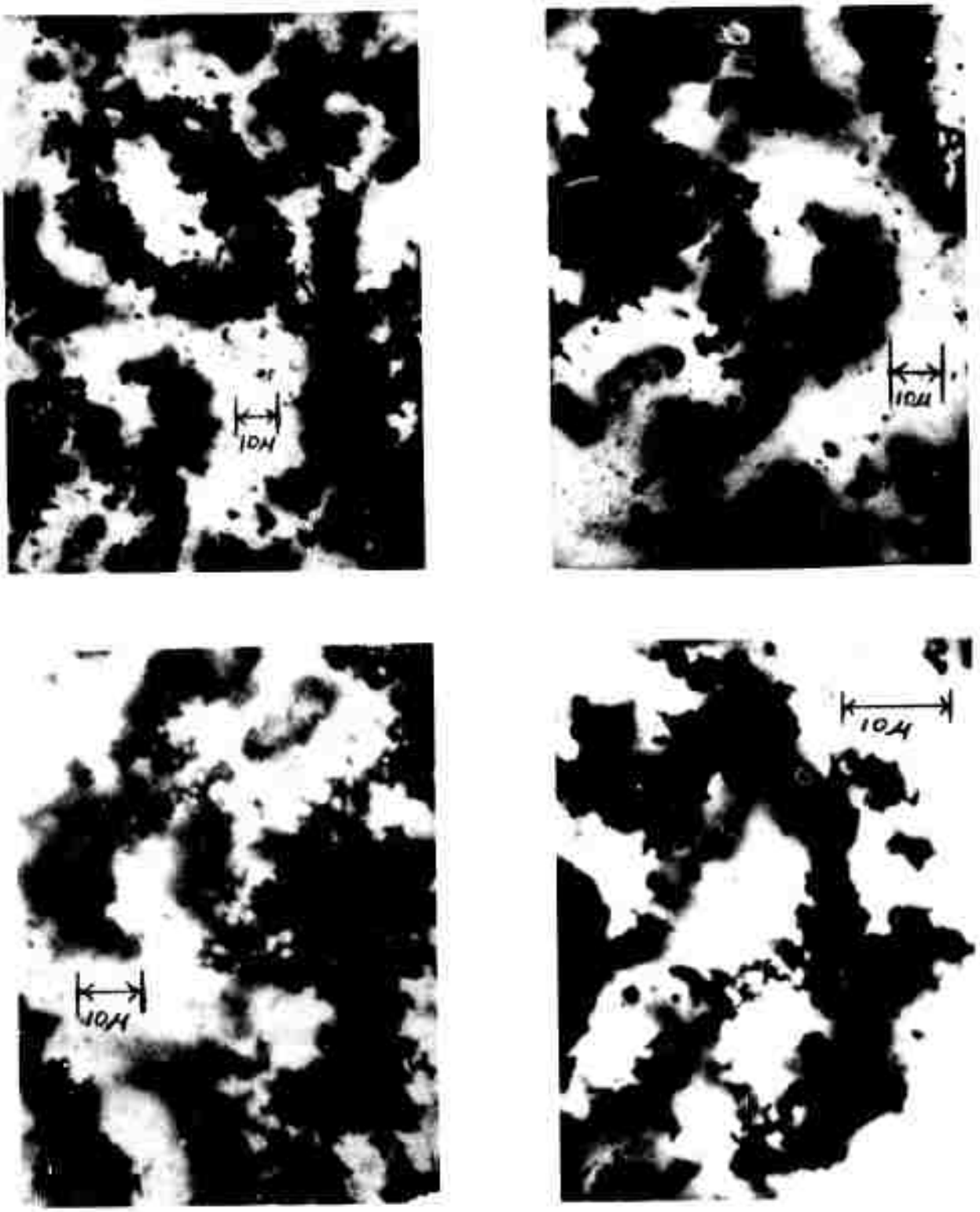

Figure 2. Resistor Microstructure: Transmitted Light

particles begin to sinter together to form the continuous network that is required for a non-insulating structure. As the firing procedure continues, the conductive sintering moves toward completion, and the glass flows to fill the remaining voids, encapsulating the network. A microstructure consisting of interconnected loops of sintered RuO_2 particles as predicted by the model (see Figure 1 of the preceeding report [2]) can be observed in all of the photomicrographs, and in some instances interconnected loops of interconnected loops can be observed. While Figures 1 and 2 by no means prove the validity of the microstructure model, they do indicate a structure of the conductive phase in a thick film resistor consistant with the predictions of the model, and give encouragement for further quantitative work along similar lines.

III. RuO_2-Glass Composites

A. General

Several authors [3,4] have contended that the stress present at the contacts between conducting phase particles in a thick film resistor is a major factor in determining the resistance, and particularly the TCR of the resistor. It has also been postulated that the stress at the contacts is due to the differences in the coefficients of thermal expansion of the conducting phase and the glass. The purpose of the experiments described in this section was to determine the contribution of this effect to the electrical properties of thick film resistors, and if possible to develop a phenomological model to relate thermal expansion to electrical properties.

Massive composites of RuO_2-glass were studied in order to eliminate any effect of the substrate. The ideal experiment would have been one in which the coefficient of linear thermal expansion (α_ℓ) of the glass was the only independent variable, but this is impossible. The best compromise was decided to be the use of lead borosilicate glasses of varying composition in order to achieve a range of α_ℓ values. In addition to chemical composition, other non-controlled variables introduced by this compromise were softening temperature, annealing temperature, viscosity, and surface tension of the glass.

B. Sample Preparation

The RuO_2 powder used had been characterized previously [1]; α_ℓ was found to be approximately 6ppm/^oC. Eight glasses were prepared for the project by Dr. J. D. Grier, Owens-Illinois, Toledo, Ohio. The composition, annealing point, and softening point for each of these glasses is given in Table I. Wet chemical analysis for boron and silicon were performed at

Table I

Composition and Properties of the Glasses

Glass	PbO(w/o) (calculated)	B_2O_3(w/o)	SiO_2(w/o)	Annealing Point (°C)	Annealing Point (°C)
71-25-4 (unground)	71.05	25.0	3.95	420	510
71-25-4	71.0	25.2	3.98	—	—
50-10-40	51.0	10.0	39.0	440	750
60-10-30	59.9	10.2	29.9	436	580
81-10-9	80.6	10.2	9.2	360	500
76-10-14	75.8	10.2	14.0	390	530
55-10-35	55.6	10.0	34.4	440	700
63-25-12	62.8	25.2	12.0	440	520
71-10-19	70.9	10.1	19.0	420	530

Battelle, Columbus Laboratories, and the lead content was obtained by difference. Very little uncertainity is introduced by this approach because the glasses were of quite high purity as evidenced by the mass spectrographic analysis (Table II). The glasses were ground in a vibratory agate (99% SiO_2) ball mill, and a sample of the 71-25-4 glass was analyzed for major constituents both before and after grinding (-325 mesh) in order to determine if any pick-up of SiO_2 occured. The 71-25-4 glass was chosen because it had the lowest silica content and hence would be most sensitive to contamination. The results shown in Table I indicate an increase of 0.03 w/0 SiO_2, but this is within the accuracy of the analytical technique. The annealing and softening points given in Table I were estimated from DTA records supplied with the glasses by Owens-Illinois.

The glass pellets to be used for thermal expansion measurements were cast in a Pt foil boat by heating rapidly to about 200°C above their respective softening points, and then cooling rapidly to room temperature. The samples were then removed from the Pt boats and annealed for 1 hour at their respective annealing points.

The glass for the RuO_2 composites was first ground with mortar and pestle to break up the larger particles. The particles were then transferred to a vibratory agate ball mill and ground until they passed through a 325 mesh screen. RuO_2 powder was mixed with the glasses in the proportion of 15:100 by weight, and the mixture wet ground in butyl carbitol for 10 minutes. After grinding, the mixture was dried at 180°C for 3 hours to remove the butyl carbitol. The soft pancake of resistive mixture which resulted was broken up, the powder packed in a cylindrical rubber mold, and isostatically pressed up to a pressure of 18,000 psi.

Table II

Mass Spectrographic Analysis of 71-25-4 Glass

Element	ppmw	Element	ppmw
Li	0.02	Y	≤ 0.05
B	High	Zr	0.3
F	< 0.3	Ru	< 0.3
Na	10.	Rn	< 15.
Mg	< 4.	Pd.	< 0.2
Al	70.	Ag	3.
Si	High	Cd	2.
P	0.2	Ba	0.5
S	2.	La	≤ 0.2
Cl	2.	Ce	≤ 0.2
K	1.	Ta	< 0.2
Ca	6.	Os	< 0.3
Sc	< 0.2	Ir	< 0.2
Ti	0.2	Pt	3.
V	< 0.07	Hg	< 0.3
Cr	1	Tl	1.
Fe	10.	Pb	High
Ni	0.5	Bi	100.
Cu	1.	Th	< 0.2
Zn	1.	U	< 0.4
Ga	< 1.		

After compacting, the pellets were placed in a boat shaped Pt foil crucible, heated at a rate of 12.5°C/min to 900°C, held at 900°C for 16 minutes, cooled at a rate of 50°C/min to the annealing point of the respective glasses, held at the annealing temperature for 1 hour, and cooled to room temperature at 50°C/min. The fired resistor pellets were hand polished to shape them roughly into parallelopipeds (about 80 mm x 30 mm x 10 mm), and grooves were made on both sides of the resistor (using a diamond saw) to help lodge four Pt wires (5 mil) to be wound across the resistor. Four circumferential bands of silver epoxy paint were painted onto the resistor along the Pt wires to serve, together with the Pt wires, as the electrodes for four terminal measurements.

C. Results and Discussion

The thermal expansion measurements were made with a fused quartz dilatometer, and analyzed by the method previously described [5]. For all runs it was found that the coefficient of the quadratic term in the expansion equation was at least three orders of magnitude less than the coefficient of the linear term from room temperature to 360°C; α_ℓ can therefore be taken as a constant for each glass. The results of these measurements and calculations are given in Table III. The α_ℓ values given in Table III are in quite good agreement for those previously reported [6] for glasses in this system.

The resistance versus temperature plots for all of the composities were quite linear over the temperature range measured (-55°C to 125°C). The normalized resistance versus temperature plots are shown in Figure 3, and the TCR for each composite is tabulated in Table III. The code letters of the composites in Figure 3 refer to the glass compositions given in Table III. No attempt was made to determine absolute resistivities.

Table III

Linear Coefficients of Thermal Expansion
of the Glasses and TCR of the Composities

Composite	Glass	α_ℓ (ppm/^oC)	TCR (ppm/^oC)
A	50-10-40	4.52	286
B	55-10-35	4.72	353
C	60-10-30	5.53	443
D	63-12-25	6.45	307
E	71-10-19	7.23	455
F	71-25-4	7.50	258
G	76-10-14	8.40	409
H	81-10-9	9.55	829

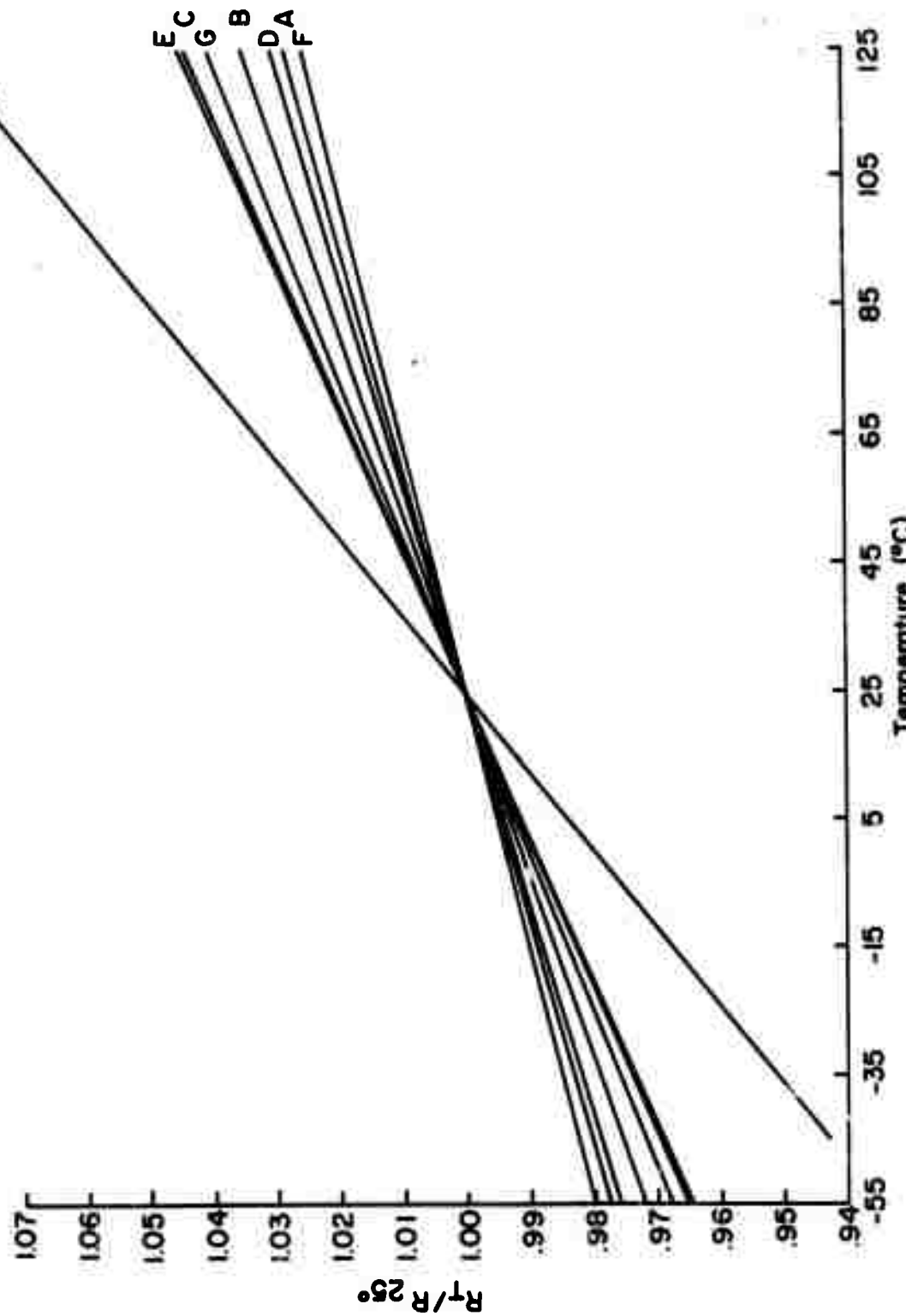

Figure 3. Normalized Resistance as a Function of Temperature for Eight RuO_2-Glass Composites

The stress (σ) on an RuO_2 particle in the composite due to the mismatch in thermal expansion is given by

$$\sigma = -K_R[\bar{\alpha}_v - \alpha_v(RuO_2)]\,\Delta T \qquad (1)$$

where K_R = bulk modulus of RuO_2

$\bar{\alpha}_v$ = average coefficient of volume expansion of the composite

$\alpha_v\,(RuO_2)$ = coefficient of volume expansion of RuO_2

ΔT = temperature change from the zero stress condition

The sign is chosen such that a positive stress represents compression, and a negative stress indicates tension. Under the conditions of this experiment ΔT is the difference between the annealing temperature of the glass and the temperature of interest. The stress on the glass is given by a similar expression, and the sum of the stresses over the volume of the composite must be zero. Therefore,

$$K_R[\bar{\alpha}_v - \alpha_v(RuO_2)]\,\Delta T\,V_R + K_g\,[\bar{\alpha}_v - \alpha_v\,(glass)]\,\Delta T\,V_g = 0 \qquad (2)$$

where V_R and V_g are the volume fractions of RuO_2 and glass ($V_R + V_g = 1$), and K_g is the bulk modulus of the glass. Solving equation (2) for $\bar{\alpha}_v$ and substituting in equation (1) gives

$$\sigma = -K_R\,\Delta T\left[\frac{K_R V_R \alpha_v(RuO_2) + K_g V_g \alpha_v(glass)}{K_R V_R + K_g V_g} - \alpha_v\,(RuO_2)\right] \qquad (3)$$

The bulk modulus of RuO_2 and the glass would not be expected to differ by more than a factor of 2; if it is assumed that $K_R = K_g$, equation (3) reduces to

$$\sigma = -K_R V_g \Delta T[\alpha_v\,(glass) - \alpha_v(RuO_2)] \qquad (4)$$

If the materials are assumed to be isotropic, $\alpha_v = 3\alpha_\ell$ and equation (4) becomes

$$\sigma = - 3K_R V_g \Delta T[\alpha_\ell(\text{glass}) - \alpha_\ell(RuO_2)] \quad (5)$$

Equation (5) predicts the simple result that the stress on the RuO_2 particles is directly proportional to the difference in coefficients of linear thermal expansion.

It has been shown [7] that the electrical resistance (R_c) of the contacts between elastic bodies is given by

$$R_c = A\, P^{-1/3} \quad (6)$$

where A is a proportionality constant and P is the pressure between contacting members. If the only force acting in the system is that due to the mismatch in thermal expansions, equation (5) can be substituted for P in equation (6) to calculate the contact resistance. This approach is valid however only for cases where $\alpha_\ell(RuO_2) > \alpha_\ell(\text{glass})$; the opposite case would predict a negative contact resistance. A comparison of the α_ℓ values for the glasses given in Table III with the α_ℓ of RuO_2 (6 ppm/°C) reveals that the inequality holds for the first three glasses but is violated for the last five. Since no drastic differences were observed between the electrical properties of composites made from the first three glasses and those made from the last five, it must be concluded that: (a) other factors are influencing the pressure on the contacts; or (b) contact resistance is not a significant factor; or (c) other variables introduced by the experimental method are dominating the results.

It was shown in the previous report (equation (16) of reference [2])

that particles of RuO_2 will be forced together by a pressure (p) given by

$$p = \gamma/a \tag{7}$$

where γ is the surface tension of the glass and a is the radius of curvature of the glass film in the neck region. If it is assumed that the pressure acting on the contacts is that given by the sum of equations (5) and (7), equation (6) becomes

$$R_c = A(p+\sigma)^{-1/3} \tag{8}$$

If p is sufficiently large then the contact resistance model is possible even for an unfavorable inequality in expansion coefficients.

The temperature coefficient of contact resistance from 25° to 125°C would be given by

$$TCR_c = \frac{R_c(125^o)-R_c(25^o)}{100\ R_c(25^o)} = \frac{R_c(125^o)}{100\ R_c(25^o)} - .01 \tag{9}$$

Since the surface tension varies only slowly with temperature it can be assumed that p is constant, and combining equations (8) and (9) gives

$$100\ TCR_c = \left(\frac{p-\sigma(25^o)}{p-\sigma(125^o)}\right)^{1/3} - 1 \tag{10}$$

If the resistance of a thick film resistor, or a composite in the present case, it taken to be the sum of the resistance of the conductive network (R_n) and the contact resistance between branches of the network (i.e. $R = R_n + R_c$), then the TCR from 25° to 125°C would be given by

$$TCR = \frac{R_n(125^o)-R_n(25^o) + R_c(125^o)-R_c(25^o)}{100\ R_n(25^o) + 100\ R_c(25^o)} \tag{11}$$

Equation (11) can be simplified to give

$$TCR = \frac{TCR_n - x\,TCR_c}{1 + x} \qquad (12)$$

where TCR_n is the temperature coefficient of the network resistance, and $x = R_c(25^\circ)/R_n(25^\circ)$.

It is possible to calculate all unknown parameters in equations (10) and (12) by using the experimental results given in Table III. However, this exercise would be futile if x and TCR_n are taken to be the same for all of the composites. This decision is based on the fact that TCR_c is a monotonic function of the difference in expansion coefficients (see equations (5) and (10)), and hence the TCR would be predicted to behave in a similar manner. The data in Table III do not show the predicted monotonic increase of TCR with α_ℓ of the glass. Only at the most extreme mismatch in expansion does there appear to be a noticable effect.

The most likely conclusions to be drawn from this study are: (a) the contact resistance between segments of the conductive network is more dependent on the surface tension of the glass and the particle size of the conductive than it is on the difference in coefficient of thermal expansion between the glass and the conductive, and (b) changes in the ratio of contact resistance to network resistance due to variations in glass properties (softening point, annealing point, surface tension, viscosity, etc.) are more important in determining the TCR of a thick film resistor than the differences in coefficient of thermal expansion between the glass and the conductive which would be expected in practice.

IV. Thick Film Firing

This phase of the project involves the continuous measurement of resistance during the firing of RuO_2 - glass thick film resistors. The intentions of these studies are fourfold: (1) to determine the onset of electrical continuity as a function of temperature at various heating rates for correlation with the sintering model; (2) to determine the onset of electrical continuity as a function of time at various temperatures for correlation with the sintering model; (3) to determine the resistance as a function of time at elevated temperatures in order to study the proposed ripening process; and (4) to prepare resistors at known stages of the firing process for subsequent microstructural investigation.

Some limited work on firing thick film resistor materials was reported earlier [1]. In that experiment a mixture of 3% RuO_2 and 97% glass was dispersed with a mortar and pestle and placed in a recessed area in an aluminum substrate with electrodes for resistance measurement. The sample resistance was $> 10^7$ Ω before firing, and about 3500 Ω with a TCR of about + 150 ppm/°C below 400°C after firing. The experiment verified that a resistor-like material could be prepared with only the most basic ingredients (RuO_2, glass, and substrate) with no additional additives or even screening agent. During the last biannum a series of similar experiments have begun using the same furnace and measuring techniques. These experiments consist of firing screen printed resistors made with varying ratios of RuO_2 to glass but no other additives except the screening agent discussed

earlier. Since the printer evaluation was in progress during this time preliminary samples were prepared with a manually operated printer.

The printing inks were prepared by first mixing the dry RuO_2 and the glass* powders with both a small spatula and a pestle in an alumina mortar. The pestle was used not for the purpose of grinding the powder to smaller size but to disperse any small agglomerates. The dispersive process can be visually observed in the low RuO_2 content mixtures that are grey in color. Subsequent dispension steps, discussed below, have shown that this method does not break up all agglomerates and so the more common precedure of using a high speed air blender would probably have worked at least as well.

The next step in the mixing was to blend the powder and screening agent. A first attempt was made with a mortar and pestle but this was obviously unsatisfactory. Because of the viscosity of the mixture a considerable amount of air was trapped, and screening and firing steps showed the dispersion was not as complete as when the ink was dispersed on the small three-roll mill. During the latter dispersion procedure, the dispersal of additional agglomerates could be seen, the ink had a smooth texture, the viscosity was lower, and the printed and dried resistors had a more uniform appearance. After this initial experiment, all inks were blended only on the three roll mill. The mixing rolls were adjusted to disperse the powder with a minimum of grinding. Inks containing 10%, 40% and 50% RuO_2 to glass were prepared in this way.

---

*The glass used for all experiments in this phase of the project was 63% PbO - 25% $B2O_3$ - 12% SiO_2, which has a coefficient of linear thermal expansion similar to both RuO_2 and the 96% alumina substrate.

After being manually screen printed onto 96% alumina (AlSiMag 614) substrates the resistors were dried at 220°C for 15 minutes followed by 45 minutes at 300°C. The object of this drying procedure was to remove a large fraction of the organic screening agent with minimum effect on the inorganic materials. The samples were then stored in a desiccated cabinet until firing.

Only preliminary results have been obtained from the firing of the resistors. One resistor from each of the 10%, 40% and 50% inks was fired through several subsequent cycles for different times and at different temperatures. No attempt has been made to correlate the results of these preliminary firings with the sintering model, but Figures 4 and 5 show the type of data obtained. Figure 4 shows the first firing cycle of a 10% and a 40% RuO_2 resistor. The 40% resistor was conductive before firing, having a resistance of 30 ohms. This resistance remained essentially constant up to the softening temperature of the glass and then decreased with increasing temperature. During the cooling portion the TCR of the resistor was about +500 ppm/C°, not small by industrial standards but small enough that the essential reactions of resistor formation must have taken place. The resistance of the 10%, RuO_2, also shown on Figure 4, was measurable prior to firing but increased rapidly to exceed the capabilities of the present measuring system before decreasing at high temperatures. The resistance decrease at high temperature has been observed before [1] and is related to the parallel conductance of the glass. During the cooling portion the resistance increases and remains high until the temperature reaches the softening point of the glass. Below 450°C the TCR is again low, about 400 ppm/C°. A presently unexplained phenomena is the non-infinite resistance before firing and the increase just below 100°C. This

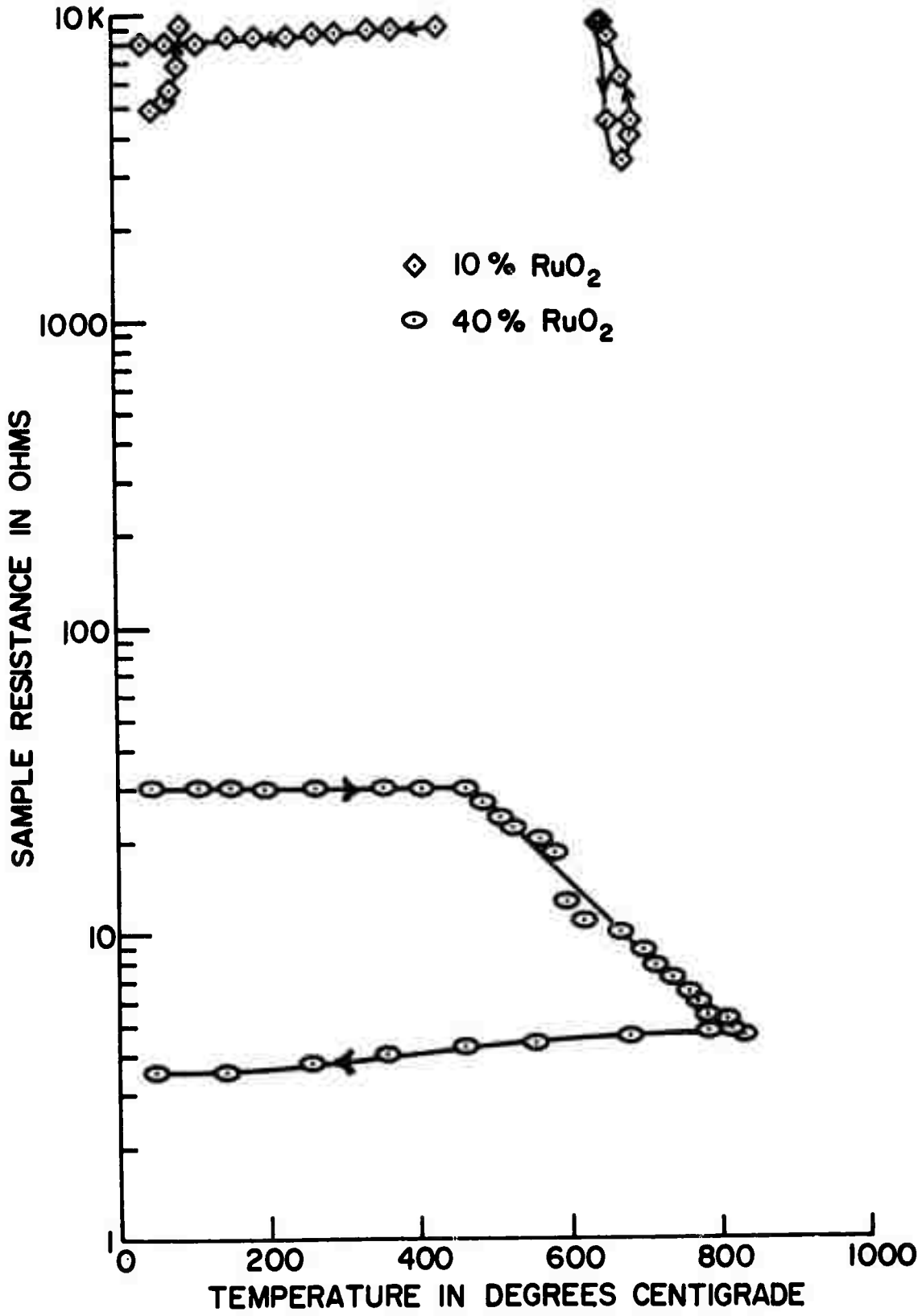

Figure 4. Resistance Changes During Thick Film Resistor Firing

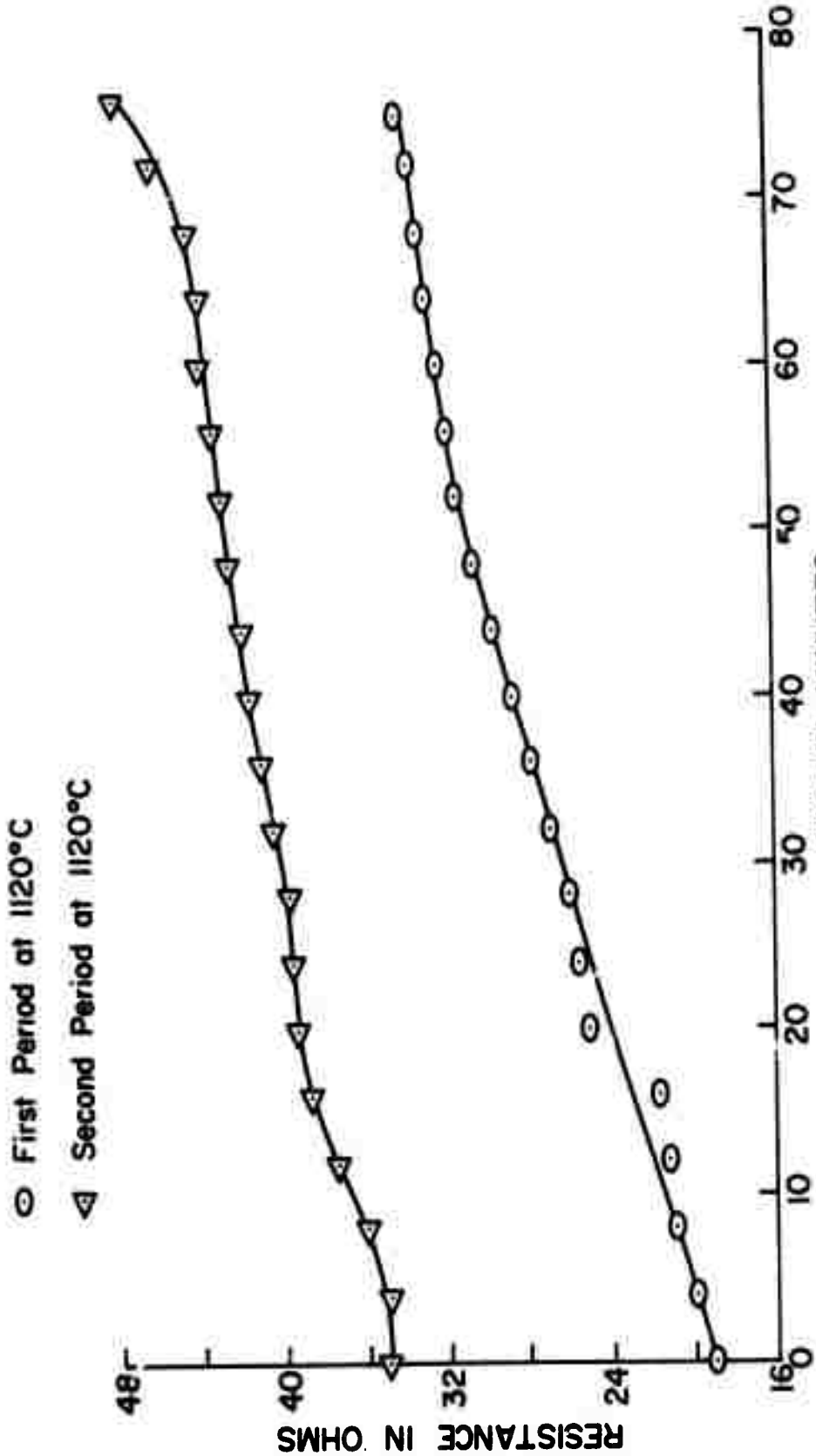

Figure 5. Isothermal Resistance Changes for a 40% RuO_2 Resistor

type of behavior has been reported earlier [8] for Pd-PdO-Ag resistors and was supected of being related to organic removal and oxidation-reduction reactions of PdO. The film represented in Figure 4 had already been dried at 300°C for 45 minutes, and RuO_2 is quite stable in this temperature range. Although all dried resistors were stored in a desicated cabinet, the temperature at which the resistance changed suggests that the resistance change may have been related to moisture picked up during sample attachments and before the initial firing.

Figure 5 shows resistance as a function of time at a constant temperature of 1120°C for the 40% RuO_2 resistor. In this case the resistance increased with time as predicted for the ripening phase of the sintering model [2]. Quantitative correlations with the model must await more complete data, but the observed behavior is encouraging.

V. Thick Film Printing

A. General

The purpose of this project is to study conduction mechanisms in thick-film resistors and conductors; however, the printing process must be studied to an extent sufficient to define its contribution to any observed variation in the final value of resistance. Numerous articles [9-12] have been written concerning the parameters that influence screen printing and some have discussed specific recommendations to improve the uniformity of deposition. However, screen printing is still more art than science and the results obtained from these studies do not provide specific instructions for setting up an arbitraty printing machine so that the printing uniformity will be optimized nor do they enable the prediction of the degree of uniformity in resistance value obtainable with optimism adjustment. Therefore, an evaluation program was undertaken to determine these two factors for the laboratory printer. The procedure was to vary one adjustment parameter at a time while all others were held as constant as possible in order to look for minima in the standard deviation of printing performance. This is discussed in greater detail after the materials and machine are described.

B. Screening Material and Apparatus

The printing ink used for the evaluation was described earlier [2] although a drafting error caused the vertical axis for Figure 12 of reference

[2] to be incorrect by a factor of 10; the viscosity at a shear rate of 1 sec^{-1} is 140 Kcps and more recent measurements have shown the viscosity to be 17 Kcps at 150 sec^{-1}. These two shear rates have been chosen as standarization points to maintain the viscosity of all printing inks as uniform as possible since viscosity is a source of printing variation. A nominal formulation consists of 40 volume percent inorganic powder and 60 volume percent screening agent made with 5 weight percent N-300 ethyl cellulose dissolved in butyl carbitol (diethylene glycol monobutyl ether) solvent. Final viscosity adjustment is done with solvent content. The printer evaluation was carried out with a glass formulation screened in a square pattern, 0.435" x 0.435", onto a 0.50" x 0.50" x 0.020", 96% alumina substrate. The average thickness of the dried film was 0.00135 inch.

The screen printing machine obtained for this project is a manual version of the Aremco 3100 shown in Figure 6a. All motions are controlled by air actuated hydraulic cylinders, and the overall mechanical construction seems to be adequately rigid and repeatable. The machine is adjustable with squeegee speeds of 1-10 ips, squeegee overtravel of 0-0.10 inches, and screen-to-substrate spacing of 0 (contact printing) to 0.10 inches. The machine as installed in the laboratory (Figure 6b) is operated with compressed nitrogen tanks because gas pressure influences the squeegee speed. The pressure is kept constant at 100 psi with a two stage regulator, and is flow stabilized with second gas cylinder that acts as a ballast tank. Several minor modifications have been made with the machine such as calibrated control for the squeegee speed adjustment, microswitches for automatic printing cycles, substrate holder, etc.

A significant modification has been made in the squeegee shape. Probably the most common squeegee shape includes a sharp printing edge and an

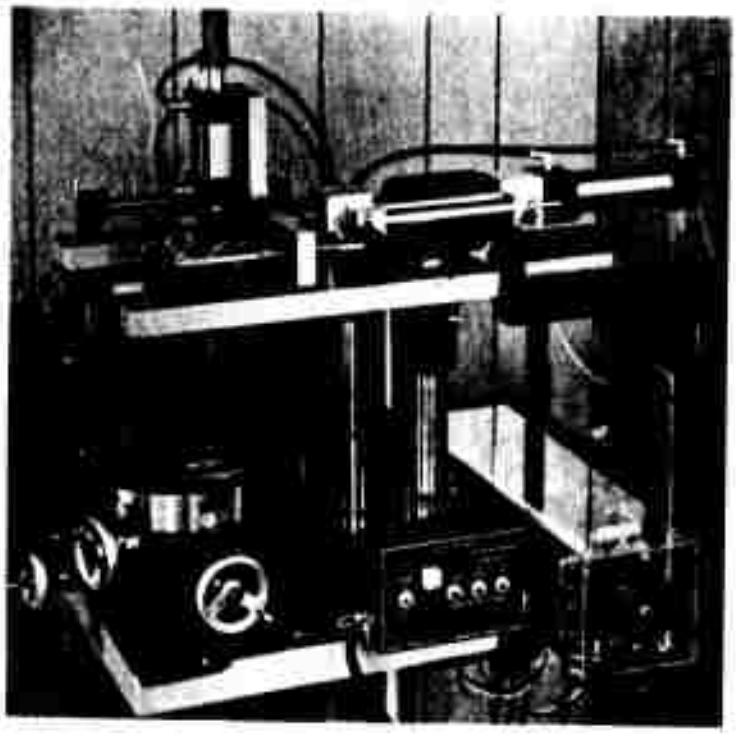

a. As Recieved

b. Installed in the Laboratory

Figure 6. AREMCO 3100 Screen Printing Machine

inclined leading surface although these two characteristics have been obtained by a variety of different methods. Figure 7a shows the shape initially selected for this project. Although the inclined leading edge is maintained, the sharp printing edge has been replaced with a 0.050 inch flat surface parallel to the top of the substrate (screen) surface. This feature was incorporated in order to reduce the rate of wear of the squeegee on the screen surface and thereby produce more uniform printing over a longer time. The basic features of the squeegee holder are shown in Figure 7b. The flat blade is held between two parallel plates with rigid spacers that limit the compression of the squeegee blade. The mechanism that holds this squeegee assembly in the machine allows limited rotation on one axis so that the long printing edge is always free to align with the screen surface.

In addition to the mechanical adjustment of the printer there are numerous other factors which influence the results associated with the printing operation. These other factors will be held constant at the values given in Table IV, and hence become boundary conditions for all subsequent critical experiments which involve printing.

C. Evaluation

The first series of experiments dealt with the repeatability of basic machine adjustments. It was determined that screen-to-substrate distance and squeegee overtravel remained constant to better than $\pm$ 0.001 inch, that there was no measureable lack of uniformity of squeegee speed near the center of the stroke, and that the squeegee speed could be repeatably set to $\pm$ 0.2 ips. These latter tests were performed with an electronic counter and mechanical contacts. The testing then proceeded to the question of repeatable deposition of ink.

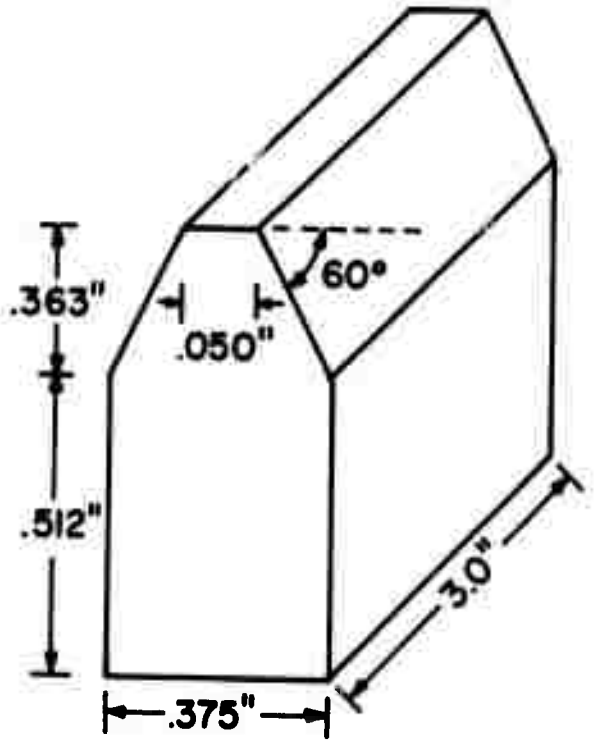

a. Squeegee Shape

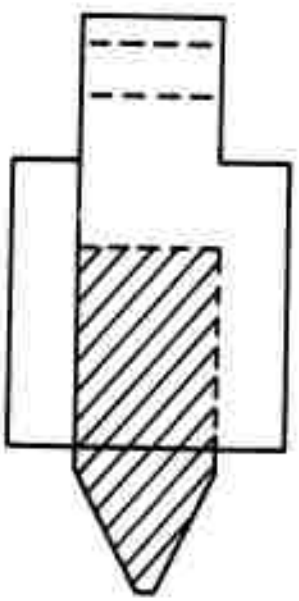

b. Squeegee Holder

Figure 7. Squeegee Design

Table IV

Boundary Conditions for AREMCO 3100

Screen	Squeegee
material - 304 stainless steel	material - polyurethane
mesh - 165	hardness - 70 durometer
wire diameter - 1.9 mil	angle of attack - 60^{o}
size - 6 3/4" x 8" I.D.	print direction - forward
weave - plain	shape - see Figure 7a
tension - 2 to 6 lbs.	holder design - see Figure 7b
emulsion type - polyvinyl alcohol	
imulsion thickness - 0.4 to 0.8 mil	

Prior studies [9-12] of the parametric dependencies of thick film screening have used criteria such as ink spread, ink thickness, ink profile, surface smoothness, and line resolution for judging optimum conditions for screening. None of these criteria are directly related to film resistance, our primary concern. The resistance (R) of a thick film resistor or conductor is given by:

$$R = \rho \frac{\ell}{A},$$

where ρ is the resistivity of the film, ℓ is the distance between conductive electrodes, and A is the cross sectional area normal to the direction of current flow (thickness times width). The weight (W) of the same film is $W=d\ \ell\ A$, where d is the density of the ink. Combining these equations gives $R = \rho \frac{\ell^2 d}{W}$. If the distance between conductive electrodes (ℓ) is constant,

$$\frac{dR}{R} = \frac{-dW}{W},$$

and the relative error in resistance is equal to the relative error in the weight of film deposited. Errors due to a non-uniform thickness were discussed in the previous report [2], and it has been assumed here that the resistor is homogeneous through its thickness. Therefore, the weight deposited was selected as the criterion for judging optimum conditions for screening. To eliminate weight changes due to solvent evaporation the screened substrates were dried at 200°C for 15 minutes to remove all of the butyl carbitol. No additional weight changes to the accuracy of the measurements (0.2 mg) could be detected for drying times up to 30 minutes.

Establishing reasonable uniformity in printing was accomplished by varying the three printing machine variables: squeegee speed, squeegee

overtravel, an screen-to-substrate distance. The machine was first adjusted to have a squeegee overtravel of 15 mils and a screen-to-substrate separation of 30 mils, values that preliminary printing showed to be adequate.

The squeegee speed was then varied from 3.0 in/sec to 8.5 in/sec. Table Va shows the average and the standard deviation (σ) in weight deposited. Figure 8a is a graphical display of these results showing percent deviation (100 σ/average weight) plotted versus squeegee speed. The graph shows an obvious (1/3) decrease in percent deviation at the higher speeds. In addition to minimizing percent deviation, it is also important that the weight deposited be independent of squeegee speed. If this is true then the weight deposited will not vary if the squeegee speed changes slightly. As can be seen from Table Va, the weight deposited is constant above 5.7 ips. Since 5.7 ips is near the center of the linear portion of the speed control adjustment, this value was chosen for further evaluation studies.

The second parameter investigated was the squeegee overtravel. Overtravel is a common industrial parameter used to specify the amount of downward pressure exerted by the squeegee during the printing operation. In this case, zero overtravel is just sufficient to depress the screen down to the substrate. Overtravel greater than zero results in the squeegee being compressed as it attempts to push the screen below the top of the substrate. The squeegee speed was set to 5.7 ips, the screen-to-substrate distance set to 30 mils, and the overtravel varied from 0 to 20 mils. Table Vb shows that immeasurable material was deposited at zero overtravel and Figure 8b shows that percent deviation decreases with decreasing overtravel but changes very little below 15 mils (the large deviation indicated

Table V

Effect of Screen Printer Parameters on Film Weight Deposited

(a) Effect of Squeegee Speed

Squeegee Speed (in/sec)	Average Weight Deposited (mg)	Standard Deviation (σ) (mg)
3.0	10.9	0.29
5.7	11.2	0.16
7.2	11.4	0.15
8.5	11.3	0.12

(b) Effect of Squeegee Overtravel

Squeegee Overtravel (mils)	Average Weight Deposited (mg)	Standard Deviation (σ) (mg)
0	0	--
5	11.9	0.13
10	11.2	0.26
15	11.1	0.14
20	10.2	0.17

(c) Effect of Screen-to-Substrate distance

S-S Distance (mils)	Average Weight Deposited (mg)	Standard Deviation (σ) (mg)
0	11.5	0.27
10	11.6	0.29
20	11.7	0.20
30	11.6	0.16
40	11.8	0.16
50	11.8	0.18

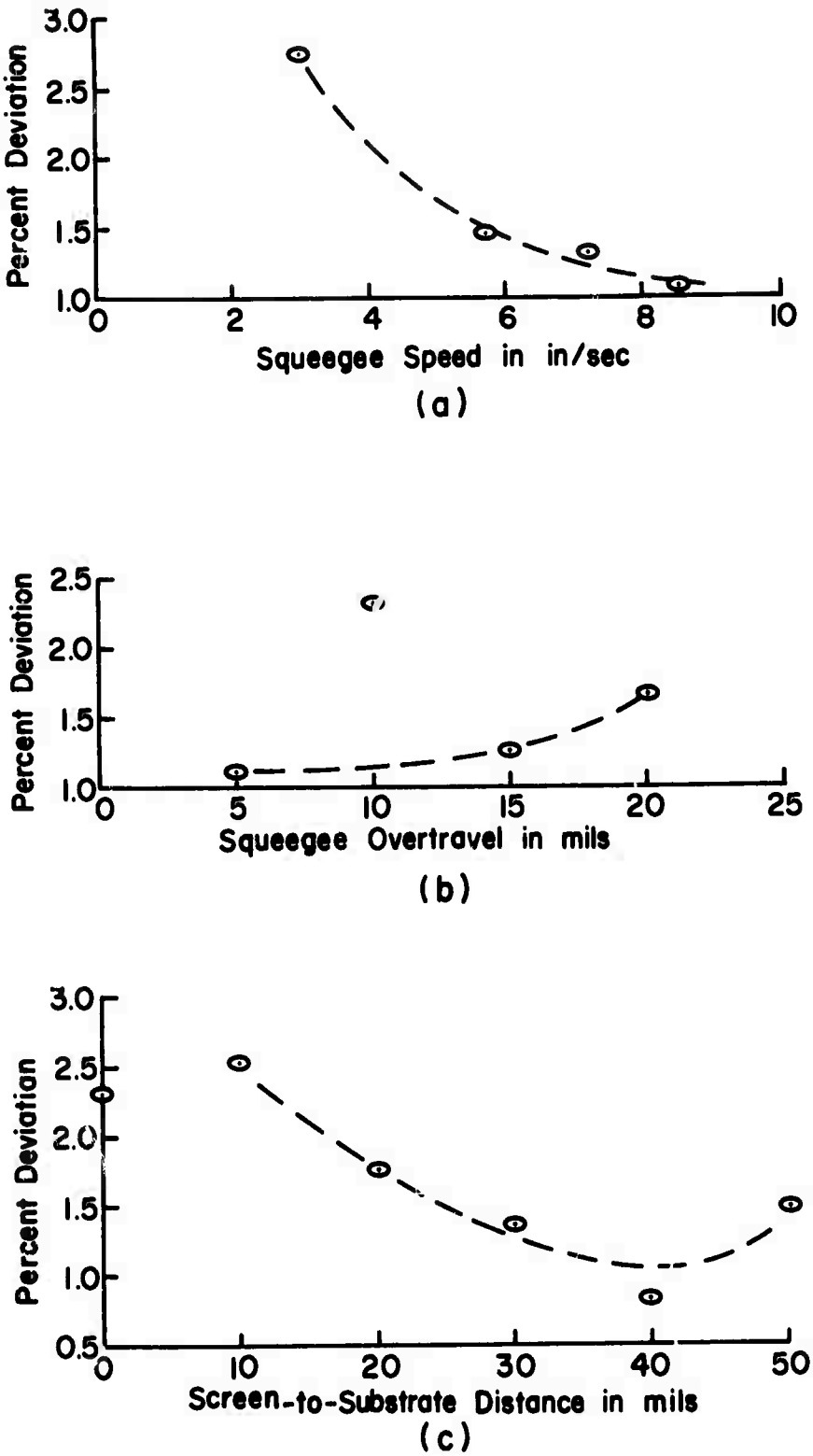

Figure 8. Effect of Screen Printer Parameters on Film Weight Deposited

at 10 mils seems to be due to the fact that there were only six samples, one of which was relatively far from the mean.) Although Figure 8b shows 5 mils overtravel to be optimum, Table Vb shows that the weight deposited varies as a function of overtravel at this setting. Therefore, 12 mils overtravel was chosen for further evaluation studies. Table Vb shows that the amount deposited is constant in this range while the standard deviation is still small. Also, it is anticipated that the deterioration of the screen will not be too rapid at this setting.

The third parameter to be optimized was screen-to-substrate distance. The squeegee speed was set to 5.7 ips, the squeegee overtravel was set to 12 mils, and the screen-to-substrate distance was varied from 0 (contact printing) to 50 mils. Table Vc shows that the weight deposited was essentially constant over the range investigated, but Figure 8c shows a minimum in the percent deviation at 40 mils. Thus, the optimum settings determined by these experiments are:

Squeegee Speed: 5.7 ips

Squeegee Overtravel: 0.012 inches

Screen-to-substrate Distance: 0.040 inches

These series of evaluation experiments were not carried out with scientific rigor. Only nine samples were used in each sample lot. The parameters could have been varied in smaller steps to obtain more date points, and after finding a tentative minimum in percent deviation the entire experiment could have been repeated, centered about the tentative minimum, as a method of fine tuning. Nevertheless, a useful scientific method has been demonstrated for systematically determining optimum adjustment and the method seems far better than the intuitive approach.

As a final test of the evaluation procedure five groups of fifty samples each were screened printed, dried, and weighed after the machine was randomly misadjusted, cleaned, and readjusted between each group. The results of these five runs were:

Run No.	Average Weight Deposited (mg)	Standard Deviation
1	11.5	0.17
2	11.3	0.22
3	11.6	0.25
4	11.8	0.23
5	11.3	0.20

Figure 9 is a histogram showing the compilation of all five runs along with the average and standard deviation.

The conclusions possible from the results of these experiments are that the (2σ) variations in resistance value due to the printing operation will be 4% about the mean for a single printing session and about 5% about the mean over many printing sessions. Resistance changes observed in any future experimental program must be greater than these values in order to be significant. Actually, the scatter in weight deposited may have been less because the variations in weight were about equal to the accuracy of the balance; if objects of identical mass were weighted the scatter would be about the same ($\pm$ 0.2 mg).

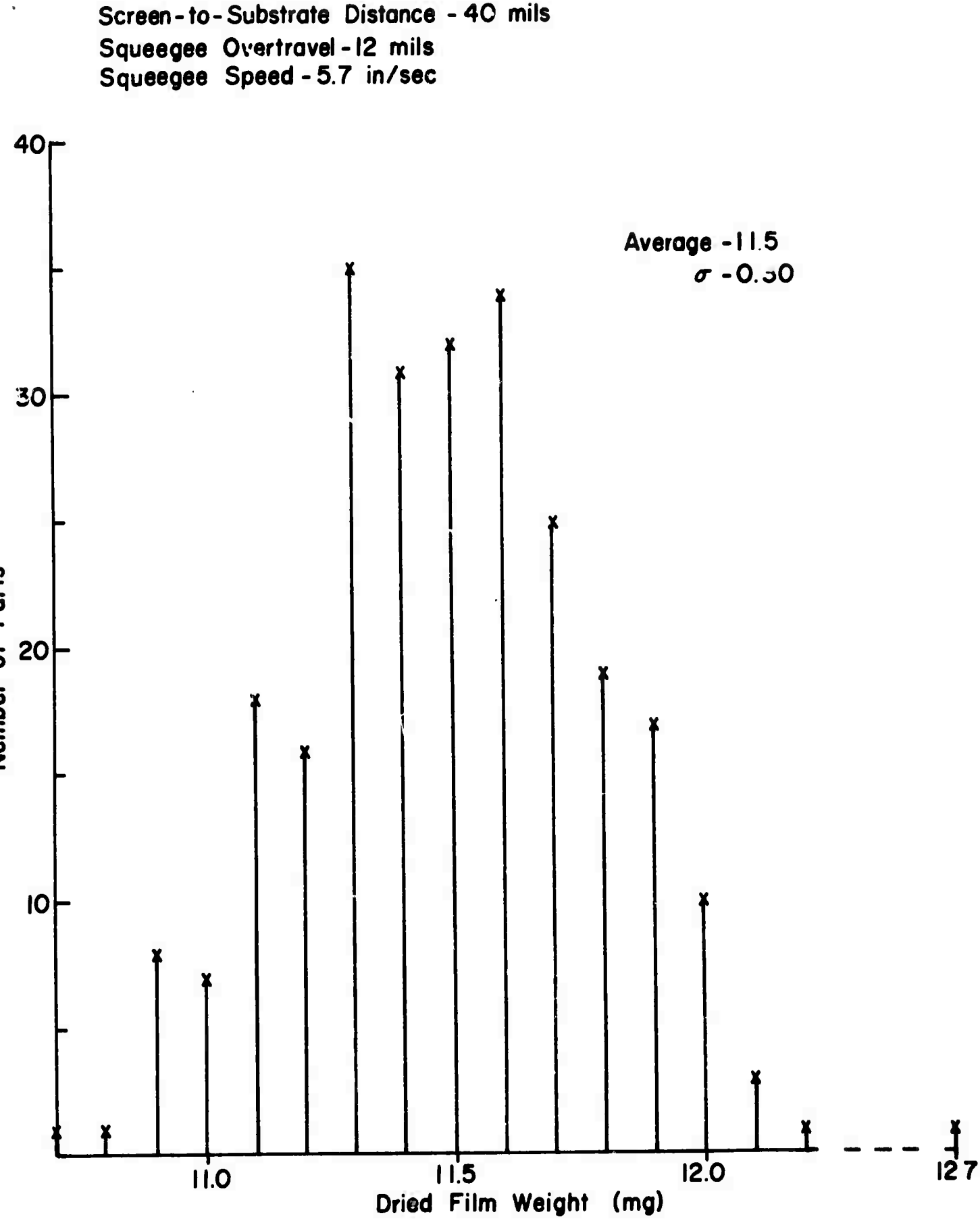

Figure 9. Variation of Film Weight

VI. Summary and Future Plans

A. The preliminary studies of resistor microstructure and resistance changes during firing have yielded results consistant with the model for microstructure development. Work along the same lines will proceed.

B. The study of RuO_2-glass composites has shown that the mismatch in thermal expansion between RuO_2 and the glass has only a minor effect on TCR as long as the difference is within reasonable limits.

C. The evaluation studies of the screen printing machine demonstrated that variations in the resistance of thick film resistors resulting from the screen printing operation will be within $\pm 4\%$ for a given printing session, and within $\pm 5\%$ over the long term.

Studies to be continued or initiated during the coming period include:

1. Sintering Studies

The steps postulated for the microstructure model will be studied. Model experiments to measure the rate of neck growth between spherical particles of both glass and RuO_2 in the presence of glass will be conducted to determine the kinetics of the various sintering processes. These measurements will be made by hot stage microscopy with spheres in the $10\mu m$ range in order to slow the kinetics to a measurable rate. The important material parameters are surface tension and viscosity of the glass, conductive-glass interfacial energy, and solubility and diffusivity of the conductive in the glass.

2. Conductive Alloy Formation

Noble alloys for conductives are often assumed to be formed during firing of a formulation containing fine powders of the pure metals. The degree of alloy formation is particularly important for alloys containing gold, silver, or palladium; pure gold and silver exhibit excessive solder leaching, and pure palladium exhibits excessive oxidation while proper alloys of these metals show a considerable reduction of these detrimental effects. High temperature x-ray diffraction techniques will be utilized to study the kinetics of alloy formation as a function of particle size. These results will then be compared with the kinetics of the sintering processes.

3. Particle Size Effects on the Resistivity of RuO_2

Previous studies on this project indicate that the apparent electrical properties of small particle size (50-100Å) RuO_2 may differ from that of the bulk, single crystal values; the electrical resistivity may be greater by a factor of about three and the TCR lower by about the same factor. A possible explanation for these phenomena is that the scattering of the conduction electrons is increased due to increased crystal defects. The procedure for determining the resistivity of the powder will be to uniformly disperse the powder in a proper matrix, measure the resistivity of the composite, and apply the proper mixing rules. A review of hetrogeneous microstructures and the associated mixing rules shows that for maximum sensitivity to the resistivity of the dispersed phase (RuO_2), the resistivity of the matrix material should not be greater than ten times the resistivity of the powder. A microstructural analysis of the cooled composite will be made to determine the degree of dispersion and grain size of the matrix.

Knowledge of these parameters is necessary for proper application of the mixing rules.

Previous measurements with single crystal RuO_2 down to 2 μm diameter have failed to show any size effects; the TCR was identical to that of more massive single crystals. Thus, size effects can only be important below this size. Using powder at least as large as 1 μm in diameter, as is planned, will allow verification of the measurement technique.

4. Electrical Properties of the RuO_2 Interface Region

Even though results reported previously indicate that the electrical properties of small particle size RuO_2 are significantly different from those of massive single crystal RuO_2, the differences are not great enough to explain the nearly-zero and sometimes negative TCR observed with thick film RuO_2 resistors. This phenomenon must be due to an additional effect resulting from the sintering process. An attempt will be made to better characterize the "contact" resistance between adjacent regions of RuO_2 in the glass by continuing the experiments with the crossed single crystals with glass at the interface and comparing the results with the RuO_2-glass composites discussed later. In some cases, the crystals will be precoated with glass before being placed in contact to insure glass in the interface. If the results of this work suggest that quantum mechanical tunneling is likely then experiments involving, for example, glass coated single crystals in mercury, will be performed in order to correctly model this conduction mechanism.

5. Microstructure of Resistors and Conductors

The details of microstructure associated with "good" resistors and conductors will be determined. Of prime importance is the identification

of the conducting phases, their shape, size, distribution, composition, and interaction.

6. Effects of Substrate Expansion

Substrates with coefficients of linear thermal expansion varying from 2 to 10 x $10^{-6}/^{o}C$ have been obtained and flame sprayed with a thin coating of alumina so that the resistor substrate interface will be the same in all cases. The resistance and TCR of resistors printed and fired on these substrates will be measured and the results analyzed in light of the results obtained with the RuO_2-glass composites.

7. Test of Models

The sheet resistance and TCR of resistors and conductors will be determined as a function of volume fraction of conductive phase to glass. and as a function of particle size of the conducting phase and of the glass. The important glass parameters (viscosity and surface tension) will be varied at constant thermal expansion, and the results compared with predictions of the microstructure model and the interface model. Chemical additives which will alter the electrical properties according to the interface model, but which will not effect microstructure development will be utilized to further test the interfact model.

VII. References

1. R. W. Vest, Semi-annual Technical Report for the period 7/1/70-12/31/70, Purdue Research Foundation Grant No. DAHC 15-70-G7, ARPA Order No. 1642, February 1, 1971.

2. R. W. Vest, Semi-annual Technical Report for the period 7/1/71-12/31/71, Purdue Research Foundation Grant No. DAHC 15-70-G7, ARPA Order No. 1642, February 1, 1972.

3. L. J. Brady, Proceedings IEEE Electronic Components Conference, 238 (1967).

4. C. J. Pukaite and G. Goodman, Bull. Amer. Ceram. Soc., 48, 428 (1969) Abstract.

5. R. W. Vest, Semi-annual Technical Report for the period 1/1/71 - 6/30/71, Purdue Research Foundation Grant No. DAHC 15-70-G7, ARPA Order No. 1642, August, 1. 1971.

6. R. F. Geller, E. N. Bunting, and A. S. Creamer, J. Res. NBS, 20, 57 (1938).

7. F. P. Bowden and D. Tabor, Proc. Roy. Soc. A, 169, 391 (1939).

8. Y. Nishimura, K. Asama, and H. Sasaki, FUJITSU Sci. and Tech. J., 4, 159 (1968).

9. L. F. Miller, Solid State Tech., p. 46, June, 1969.

10. B. M. Austin, Solid State Tech., p. 53, June, 1969.

11. D. R. Kobs and D. R. Voigt, Solid State Tech., p. 34, February, 1971.

12. R. W. Atkinson, Solid State Tech., p. 51, May, 1971.